Co-deposition integrating with interfacial polymerization to prepare PA/PDA/PVDF nanocomposite membrane and the application in the simulating RB5 dyeing wastewater treatment

Heng Cui, Zhehui Li, Jun Wang*, Honghai Yang*

College of Environmental Science and Engineering, Donghua University, Shanghai 201620, China, emails: wangj@dhu.edu.cn (J. Wang), yhh@dhu.edu.cn (H.H. Yang), 1763515641@qq.com (H. Cui), 1083761413@qq.com (Z.H. Li)

ABSTRACT

Polyamide (PA)/polydopamine (PDA)/poly(vinylidene fluoride) (PVDF) nanocomposite membranes were prepared by the method of dopamine (DA)/polyethyleneimine (PEI) co-deposition integrating with interfacial polymerization (IP) with trimesoyl chloride. Fourier transform infrared spectrometer, scanning electron microscopy, atomic force microscopy and water contact angle were used to characterize the PA/PDA/PVDF nanocomposite membranes. Effects of the co-deposition time, the mass ratio of DA to PEI, the molecular weight of PEI and the content of DA + PEI on the morphologies and roughness of the membrane surface, the cross-section of the selective layer and the performance of the PA/PDA/PVDF nanocomposite membranes were investigated. Results showed that the co-deposition time has significant effect on the rejection of PA/PDA/PVDF nano-composite membranes, the other three factors have few effects on the rejection. All the four factors have remarkable effects on the permeation of the PA/PDA/PVDF nanocomposite membranes. When the rejection of PEG1000 and RB5 was 99%, the permeation of water and reactive black five (RB5) dyeing wastewater was 16.67 and 8.2 L m^{-2} h^{-1} bar^{-1}, respectively. The water flux and the RB5 dyeing wastewater permeation of the PA/PDA/PVDF nanocomposite membranes were 31.14 and 15.03 L m^{-2} h^{-1} bar^{-1}, respectively, when the PEG1000 and RB5 rejections were above 90%. Results above showed that the PA/PDA/PVDF nanocomposite membranes developed in this paper possess the potential application value in the dyeing wastewater treatment and reclamation

Keywords: PA/PDA/PVDF; Nanocomposite membranes; Co-deposition integrating with IP; DA/PEI; Dyeing reclamation

1. Introduction

Due to the toxicity and difficulty to degrade, the treatment and reclamation of dyeing wastewater have always been a concern in the field of wastewater treatment [1,2]. The nanofiltration membranes not only can recover dyes with high efficiency but also have the merits of energy-cost, compact equipment, simple in operation. So the nanofiltration membranes were used more and more widely in the dyeing wastewater treatment.

With the wide application of nanofiltration membranes, developing new kinds of nanofiltration membranes attracted intense attention. Presently, researching of the composite nanofiltration membranes was focused on developing new kind of nanofiltration membranes. The composite nanofiltration membranes were comprised of selective layer and base membranes or support layer. The selective layer and support layer can be prepared and optimized separately, therefore it is easy to tune the structure and performance of the nanocomposite membranes.

* Corresponding authors.

The flux, separation efficiency and operation stability of the nanocomposite membranes were depended on the thickness, the porosity, the physical and chemical property of the selective layer namely the roughness of the surface and the adhesiveness of the selective layer. Among these factors, the adhesiveness of the selective layer is the most significant. Once the selective layer gets peeled off from the support layer, the separation efficiency of the nanocomposite membranes will decrease dramatically and the permeation maybe surge. So how to make the selective layer stick on the base membrane surface is one of the most important for the nanocomposite membranes preparation.

The reported preparation methods of nanocomposite membranes were interfacial polymerization [6,11–14,16,17], deposition or co-deposition [3–5,7–10,15,18–28] and deposition or co-deposition integrating with interfacial polymerization [29–35]. The selective layer prepared by interfacial polymerization, usually be polyamide (PA) with strong hydrophilicity, would detach easily from the support layer, which would affect the separation efficiency and stability of the nanocomposite membranes immensely. In order to obtain adhering functional selective layer, dopamine (DA) was deposited on the support layer. DA, a mussel-inspired material, can self-polymerize to form a thin, surface-adherent poly(dopamine) (PDA) and cross-link with other materials containing amido by Michael addition or Schiff base reaction under oxidizing conditions [5,9,10,18,19–21,24,26–36]. However, the self polymerization of DA costed time too long, usually up to 24 h, furthermore, PDA inclined to agglomerating. In order to solve the problems above, researchers co-deposited $GuSO_4/H_2O_2$ and polyethyleneimine (PEI) with DA. $GuSO_4/H_2O_2$ triggered the self polymerization of DA, which made the polymerization time short from 12–24 h to 1 h. On the other hand, PEI can not only hinder the agglomeration of PDA but also enhance the hydrophilicity of the selective layer. Up to now, the base membrane materials, being used to prepare the nanocomposite membranes, were mainly poly(ether sulfone) (PES) [3,6,7,11,14,17,19,34], polysulfone (PSF) [12,13,22,29,33], polyacrylonitrile (PAN) [4,9,15,16,18,30], polyvinylidene difluoride (PVDF) [8,10,24–26,28].

Because of its excellent mechanical property, corrosion resistance, chemical stability and good membrane forming, PVDF membrane attracted great attention in the field of nanocomposite membrane development. Sakarkar et al. [8] used polyvinyl alcohol (PVA)/nano particle titanium dioxide (TiO_2) and glutaraldehyde (GA) to prepare PVDF nanocomposite membranes by interfacial polymerization. The prepared PVDF membranes were tested in the dyeing wastewater treatment. Ma et al. [10] prepared PVDF nanocomposite membranes using DA and polypyrrole (Ppy) by co-deposition method and the dyeing wastewater treatment efficiency of the prepared PVDF nanocomposite membranes were also tested. In order to separate the mixture of oil and water, Xiang et al. [24] prepared PDA/PVDF nanocomposite membranes by co-deposition of DA on the surface of PVDF ultra-filtration membranes, Shi et al. [25] prepared PDA/TiO_2/PVDF nanocomposite membranes by co-deposition of DA and TiO_2, Zin et al. [26]. Li et al. [35,36] proposed the method of inkjet printing of polyphenols (catechol (CA) or tannic acid (TA)) and sodium periodate

(SP) on a polyvinylidene fluoride (PVDF) membrane to prepare PVDF nanocomposite membranes. Literatures above mentioned stated that PVDF nanocomposite membranes were prepared mainly by interfacial polymerization, deposition and co-deposition method. Deposition or co-deposition combining with interfacial polymerization to prepare PVDF nanocomposite membranes were reported very little.

Co-deposition integrating with interfacial polymerization can couple the merits of the selective layer prepared by interfacial polymerization with that of which prepared by co-deposition. Studies regarding the co-deposition integrating with interfacial polymerization to prepare nanocomposite membranes have been reported as follows. Song et al. [28] prepared PEI/PDA/PVDF nanocomposite membranes by co-deposition of DA and PEI. Ji et al. [31] using DA and TMC to prepare PA/PDA/PVDF membranes by deposition combining with interfacial polymerization for dehydration of isopropanol. Zhu et al. [30] prepared PA/PDA/PAN nanocomposite membranes by Cu^{2+}/H_2O_2 inducing DA and PIP fast co-deposition then interfacial polymerization with TMC. Lv et al. [32] prepared poly(acrylonitrile-acrylamide-sodium acrylate) hydrolyzate (HPAN) nanocomposite by co-deposition of DA and PIP then interfacial polymerization with GA in order to concentrate salt water solution. Li et al. [33] prepared PSF nanocomposite membranes by co-deposition of DA and PIP first then polymerized interfacially with three different kinds of crosslinking agents epichlorohydrin (ECH), toluene diisocyanate (TDI) and GA to separate the mixture of salt and water. Li et al. [34] co-deposited DA and PIP then polymerized interfacially with TMC to prepare PA/PDA/PES nanocomposite membranes. Summarized upon the above literatures, the research about co-depositing DA and PEI then polymerized interfacially with TMC to prepare PA/PDA/PVDF has not been reported till now.

In this paper, in order to develop new nanocomposite membranes that can be applied in the dyeing wastewater treatment, PA/PDA/PVDF nanocomposite membranes were prepared by co-depositing DA and PEI on the surface of PVDF ultra-filtration membrane integrating with polymerized interfacially with TMC. Furthermore, PA/PDA/PVDF nanocomposite membranes were characterized by Fourier transform infrared spectrometer (FTIR), atomic force microscopy (AFM), scanning electron microscopy and water contact angle testing. The influence of co-depositing time, the ratio of DA to PEI, the PEI molecular and the content of DA and PEI were investigated at the same time. Finally, the performance and the operating stability in the simulated reactive black five (RB5) wastewater treatment of the prepared PA/PDA/PVDF nanocomposite membranes were discussed.

2. Materials and methods

2.1. Materials

PVDF (F904) were purchased from Shanghai organic Fluorine Materials Co., Ltd. N,N-Dimethylacetamide (DMAc, AR), copper sulfate pentahydrate ($CuSO_4·5H_2O$, 99%), hydrogen peroxide (H_2O_2, 30%), n-hexane (AR), dopamine hydrochloride, polyethyleneimine (PEI; 600; 800; 1,800;

1,000), polyvinyl pyrrolidone (PVP K30) polyethyleneglycol (PEG1000) all were purchased from Sinopharm Chemical Reagent Co., Ltd. Trimesoyl chloride (TMC, 98%) was obtained from Shanghai TITAN Technology Co., Ltd. Tris-HCl buffer solution (pH = 8.5) was obtained from Shenggong Bioengineering Co., Ltd.

2.2. Fabrication of PA/PDA/PVDF nanocomposite membranes

2.2.1. Preparation of base membranes (PVDF ultra-filtration membranes)

PVDF ultrafiltration membranes were prepared by the method of non-solvent induced phase separation (NIPs). Briefly, the casting solution of the PVDF powder (18 wt.%) and PVP (4 wt.%) was prepared using DMAc as solvent, and kept under constant mechanical stirring at certain temperature till a homogeneous solution is obtained, then made to stand for deaeration. After completing the deaeration, the homogeneous solution was casted on a glass plate, and then, the cast film along with the glass plate was gently immersed in the distilled water till the as-prepared PVDF membranes peel off the glass plate. The fabricated membrane was completely washed with distilled water in order to remove the remaining solvent and stored properly in distilled water containing 0.1% formalin solution to avoid microbial growth.

2.2.2. Preparation of base membranes (PVDF ultra-filtration membranes)

Fig. 1 presents the fabrication process of PA/PDA/PVDF nanocomposite membranes.

The self-made PVDF membranes were rinsed by deionized (DI) water for 24 h and then used as support for the nanocomposite membranes. Dopamine hydrochloride was dissolved in tris-HCl buffer solution (10 mL, pH = 8.5) containing $GuSO_4 \cdot 5H_2O$ (0.024 g), then dropped in H_2O_2 (30%, 40 μL), finally mixed with PEI water solution (10 mL). The circular pieces of PVDF membranes with diameter of 8 cm were fixed in a glassware and prewetted by ethanol for 30 min, and then the PVDF membranes were immersed in the fresh prepared dopamine/PEI solution and shaken at 25°C for certain time. The as-prepared membranes (PDA/PEI-modified membranes) were washed by DI water for several times and dried at room temperature.

The cross-linker, TMC (1 g), was dissolved in n-hexane (1 L). Afterwards, the PDA/PEI-modified membranes were immersed into it for 5 min at room temperature then the as-prepared PA/PDA/PVDF nanocomposite membranes were dried in the atmosphere. Finally, the obtained NFMs were rinsed several times and stored in DI water for further characterization and evaluation. The influence of co-depositing time, the ratio of DA to PEI, the PEI molecular and the content of DA and PEI was investigated

2.3. PA/PDA/PVDF nanocomposite membrane characterization

The chemical structures of DA, PEI, PVDF and PA/PDA/PVDF nanocomposite membrane surfaces were investigated by FTIR (FTS-6000), respectively. Operational details of some characterization items can refer to the literatures [38–42]. The spectra were collected from 400 to 4,000 cm^{-1} by cumulating 32 scans at a resolution of 4 cm^{-1}. The surface and cross sectional morphologies of the membrane selective layer was observed and investigated by the field emission scanning electron microscopy (FESEM, Hitachi, S4800, Japan). The membranes were dried and fractured in liquid nitrogen to prepare sectional samples. AFM (Agilent 5500) was used to analyze the surface roughness of the membrane. Small squares (approximately 1 cm^2) of the membrane samples were glued on a metal substrate. The membrane surfaces were examined in tapping mode and in a scan size of 20 μm × 20 μm. The surface roughness of the membrane was measured in terms of the mean roughness (Ra). Hydrophilicity of the membrane surface was measured by water contact angle measured by a DropMeter A-200 contact angle system (MAIST Vision Inspection & Measurement Co., Ltd., China). A drop of water (5 μL) was placed onto the sample surface and the digital image of the droplet was immediately recorded. Static contact angles were determined from these images. Contact angle reported in this study represents the mean value of more than 10 measurements at different points for each membrane sample.

2.4. PA/PDA/PVDF nanocomposite membrane performance

PA/PDA/PVDF nanocomposite membrane performance in terms of permeation flux and rejection of PEG1000 were investigated using an ultra-filtration cup (MSC300) with stirring to simulate cross-flow. The resulting membrane with an effective area of 37.625 cm^2 was subjected to
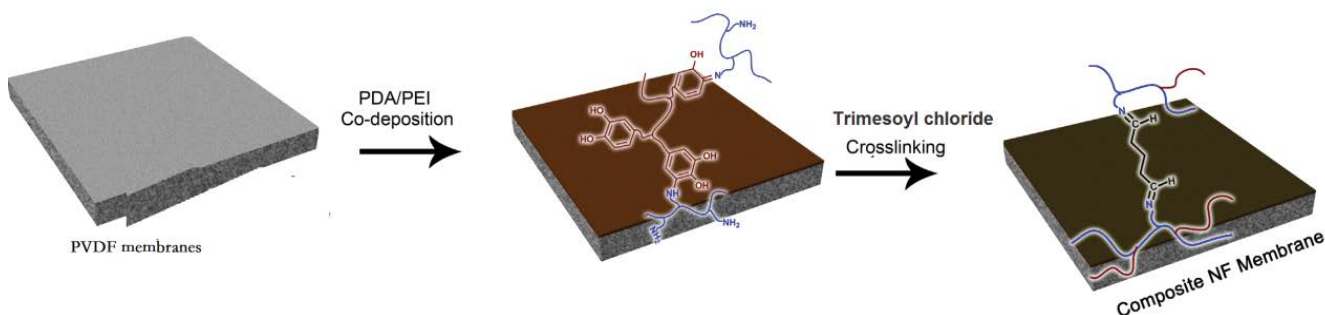

Fig. 1. Schematic diagram of the preparation process of PA/PDA/PVDF nanocomposite membranes.

pressurization with DI water at 0.15 Mpa for 0.5 h prior to filtration experiments at room temperature (20°C). The concentration of the solution was measured by total organic analyzer (TOC 5000A), respectively. Permeation flux, J, and rejection, R, were calculated according to Eqs. (1) and (2), respectively:

$$J_W = \frac{V}{(At)} \tag{1}$$

$$R = 1 - \frac{C_p}{C_f} \tag{2}$$

where V is the total volume of permeate during the operating time, t; A represents the membrane area, and C_p and C_f are the concentrations of the permeate and feed PEG1000 solution, respectively.

2.5. PA/PDA/PVDF nanocomposite membrane performance in the simulating RB5 dyeing wastewater treatment

The testing method and equipment of the PA/PDA/PVDF nanocomposite membrane performance in the simulating RB5 dyeing wastewater treatment, in terms of the simulating RB5 dyeing wastewater permeation, the RB5 rejection and the flux stability, were the same as that of the water flux and PEG1000 rejection. The time of the flux stability testing was 6 h. The concentration of the feed RB5 dyeing solution was 0.1 g/L. The concentrations of the feed and permeate of the RB5 dyeing solution were measured by UV-visible spectrophotometer (UV-7504PC). The RB5 rejection could be calculated by Eq. (2).

3. Results and discussions

3.1. Chemical structures of PA/PDA/PVDF nanocomposite surface

FTIR/ATR was used to analyze the chemical structures of the membrane surfaces and the results are exhibited in Fig. 2. Spectrum of the PVDF membrane shows that the
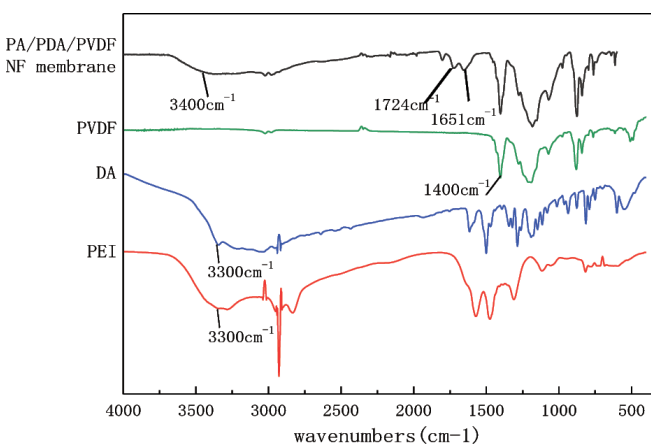

Fig. 2. Fourier transform infrared spectra of DA, PEI, PVDF and PA/PDA/PVDF.

C-F stretching vibration peaks at 1,400 cm^{-1}. After PDA/PEI co-deposition and interfacial polymerization, new peaks arise around 3,400 cm^{-1} owing to the O–H stretching vibration, new peak at 1,724 cm^{-1}, which is ascribed to the C=O stretching vibration, new peak at 1,651 cm^{-1}, which is owing to the overlapping of the C=C vibration in the aromatic and the C–N stretching vibration in the PA, which is the product of the interfacial polymerization between PDA and TMC and PEI and TMC.

3.2. Effects of DA/PEI co-deposition time on the morphologies and performance of the PA/PDA/PVDF nanocomposite membranes

Fig. 3 displays the effects of DA/PEI co-deposition time on the morphologies of the surface and cross-section and the roughness of the surface of the PA/PDA/PVDF nanocomposite membranes at the condition of PEI800, the ratio of DA to PEI 1:1, the content of DA + PEI 2 g L^{-1}. Fig. 3 shows that with the increase of co-deposition time, the agglomeration of PDA decreased (Fig. 3a), the thickness of the selective layer n increased (Fig. 3b) and the roughness of the surface decreased (Fig. 3c). These changes ascribed to PEI hinder the agglomerating of the PDA more completely and more DA/PEI co-deposit on the surface of the PVDF membrane with the increase of the co-deposition time. The effects of DA/PEI co-deposition time on the performance of PA/PDA/PVDF nanocomposite membranes are displayed in Fig. 4. From Fig. 4a it can be found that the water flux decreased dramatically from 70.7 to 16.7 L m^{-2} h^{-1} bar^{-1} while the rejection of PEG1000 increased from 80% to 99% with the co-deposition time increased from 20 to 60 min, this was because the thickness of the deposition layer increased with the deposition, after interfacial polymerization with TMC then a dense selective layer was obtained, which resulted in the increase of the membrane filtration resistance significantly. However with the deposition time extended from 60 to 100 min, the water flux increased fastly from 16.7 to 83.3 L m^{-2} h^{-1} bar^{-1} but the PEG1000 rejection decreased from 99% to 52% drastically. It was maybe because of the occurrence of the agglomeration of PDA with the deposition from 60 min then on made the interfacial polymerization with TMC unevenly, which resulted in the porous and hydrophilic selective layer. So the water flux increased quickly and the PEG1000 rejection decreased substantially. Considering both of the water flux and the PEG1000 rejection performance for the PA/PDA/PVDF nanocomposite membranes, 40 min is chosen as the optimum deposition time.

3.3. Effects of mass ratio of DA to PEI on the morphologies and performance of the PA/PDA/PVDF nanocomposite membranes

Fig. 5 displays the effects of the mass ratio of DA to PEI on the morphologies of the surface and the cross-section and the roughness of the surface of the PA/PDA/PVDF nanocomposite membranes at the condition of PEGI800, the co-deposition time 40 min, the content of DA + PEI 2 g L^{-1}. Fig. 5 shows that with the decrease of the mass ratio of DA to PEI, the agglomeration of PDA (Fig. 5a), the thickness of the selective layer (Fig. 5b) and the roughness of the surface (Fig. 5c) all decreased with the mass ratio of DA to PEI decreased from 1:1 to 1:3. This phenomenon was due to
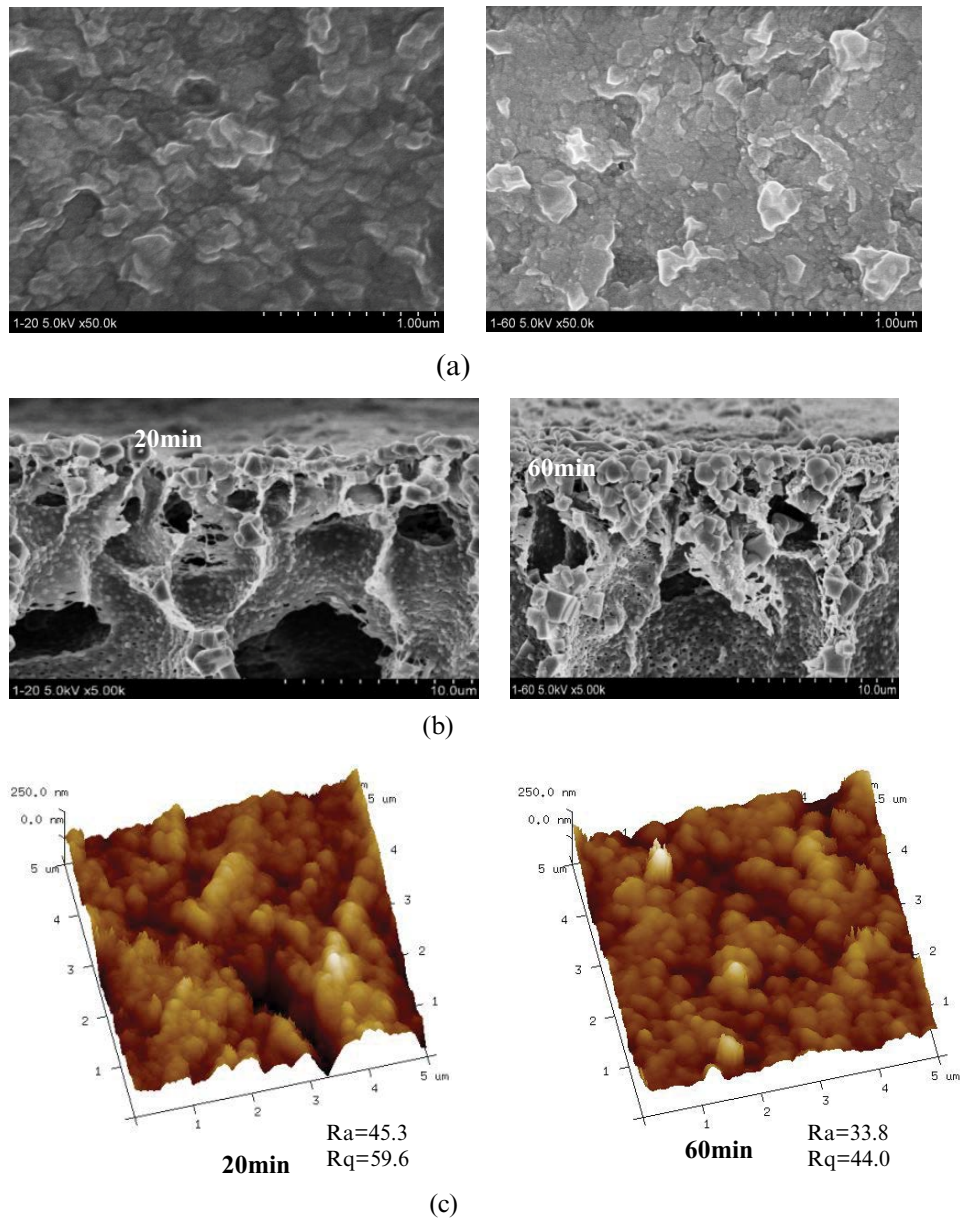
(a)

(b)

(c)

Fig. 3. Effects of co-deposition time on the morphologies of (a) the surface and (b) the cross-section and (c) the surface roughness of PA/PDA/PVDF nanocomposite membranes (SEM, AFM).
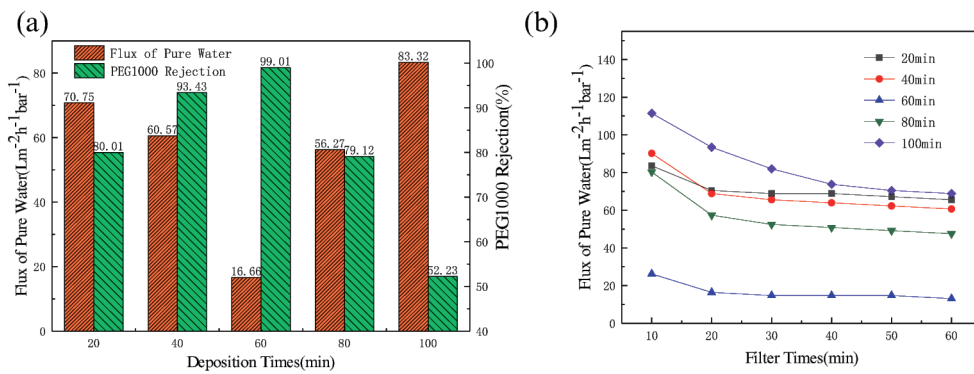

Fig. 4. Effects of co-deposition time on the performance of PA/PDA/PVDF nanocomposite membranes: (a) the water flux and PEG1000 rejection and (b) the variety of the water flux with time.
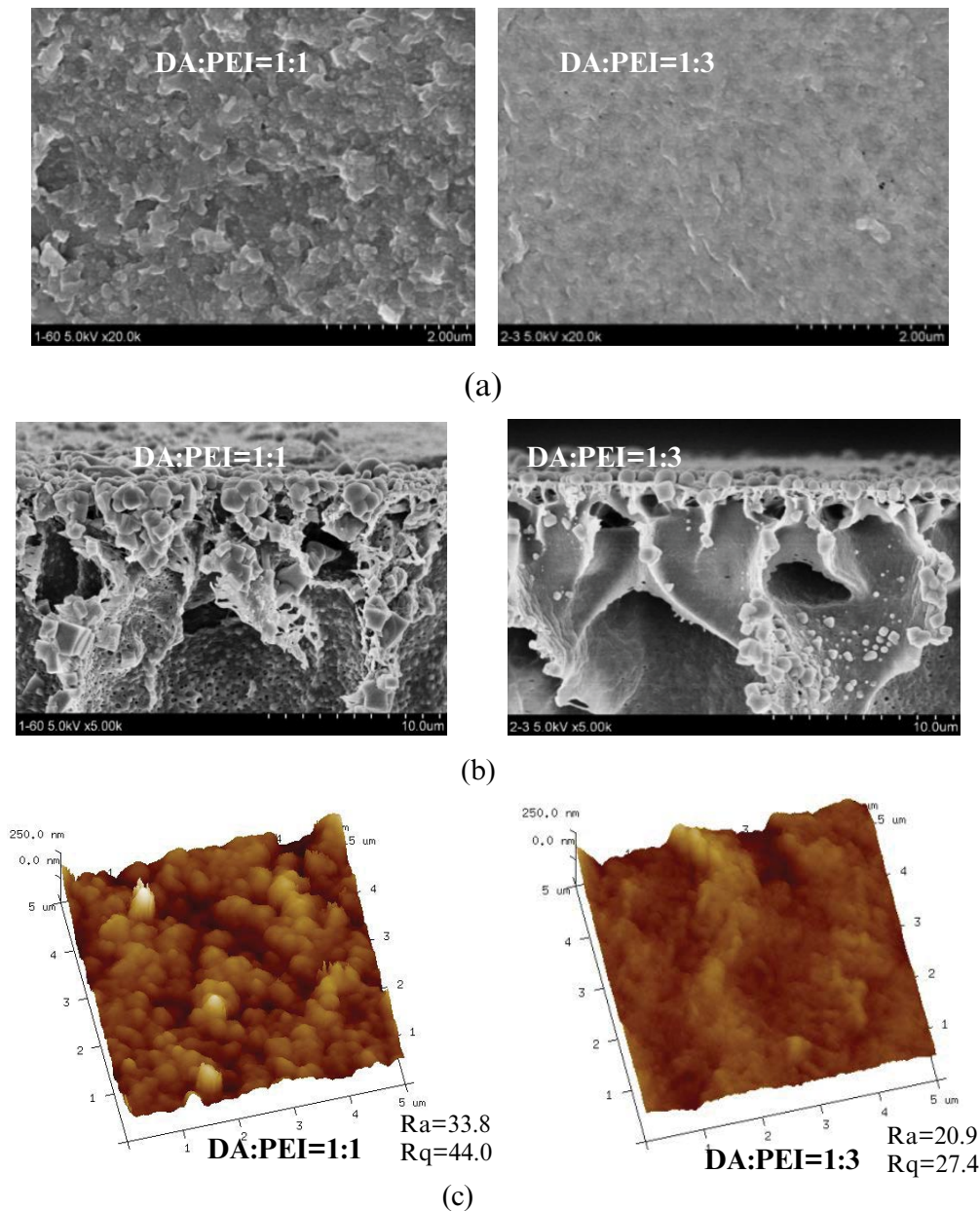
(a)

(b)

(c)

Fig. 5. Effects of the mass ratio of DA to PEI on the morphologies of (a) the surface and (b) the cross-section and (c) the surface roughness of PA/PDA/PVDF nanocomposite membranes.

the PEI content increase with the mass ratio of DA to PEI decreased, which made the PEI hinder the PDA agglomerating more effectively, at the same time, made the interfacial polymerization of TMC with PEI more completely, so the more PA was obtained leading to the surface be more smooth and hydrophilic and the selective layer be more thin. This result was coincident with that of reference [33].

The surface water contact angle and the performance of the PA/PDA/PVDF nanocomposite membranes are displayed in Figs. 6 and 7, respectively. From Fig. 6 it can be found that with the decrease of mass ratio of DA to PEI from 2:1 to 1:3, the water contact angle decreased from 62°C to 50°C, which means the hydrophilicity of the surface increased substantially. This was because with the decrease of mass ratio of DA to PEI, the PEI content increased, which means the more hydrophilic PA would be obtained leading to the enhancement of the surface hydrophilicity after the interfacial polymerization with TMC. The results of Fig. 7 show that the water flux increased significantly and the PEG1000 rejection changed little with the decrease of mass ratio of DA to PEI. The increase of the flux was due to the thickness of the selective layer became thinner and the hydrophilicity of the surface enhanced, which resulted the filtration resistance decreased significantly. While the PEG1000 rejection has little change stated that the PEG1000 rejection had no relationship with the mass ratio of DA to PEI but had intimate relationship with the co-deposition time as discussed above.

3.4. Effects of the molecular PEI on the morphologies and performance of the PA/PDA/PVDF nanocomposite membranes

The effects of the molecular PEI on the morphologies and performance on the PA/PDA/PVDF nanocomposite membranes at the condition of co-deposition time of 40 min, the mass ratio of DA to PEI 1:1 and the content of DA + PEI 2 g L^{-1} are displayed in Figs. 8 and 9, respectively. From Fig. 8 it can be found that particles decreased and the surface became smooth (Fig. 8a), both the thickness of the selective layer (Fig. 8b) and the roughness of the surface (Fig. 8c) decreased. This phenomenon was ascribed to the molecular chains of the PEI increase with the PEI molecular, which lead to the cross-linking degree between PEI and DA, PEI and TMC increasing, therefore resulted in the more smooth surface and the thinner selective layer. Fig. 9 shows that the flux decreased from 21.04 to 8.74 L m^{-2} h^{-1} bar^{-1} and the PEG1000 rejection varied a little when the PEI molecular weight increased from 800 to 10,000. It was because that the longer the molecular chain the higher the cross-linking degree of PEI with TMC and DA, which resulted the selective layer became thinner but denser, therefore leading to the decrease of the flux but little changes of the PEG1000 rejection.

3.5. Effects of the content DA + PEI on the morphologies and performance of the PA/PDA/PVDF nanocomposite membranes

Figs. 10 and 11 show the effects of the content DA + PEI on the morphologies and performance on the PA/PDA/PVDF nanocomposite membranes at the condition of co-deposition time 40 min, the mass ratio of DA to PEI 1:1 and the molecular weight PEI 800, respectively.

Fig. 10 shows that the surface tended to be more smooth and less particles (Fig. 10a), the selective layer became thicker and more porous (Fig. 10b) and the roughness of the surface decreased with the content of DA + PEI changing from 2 to 4 g L^{-1}. These phenomenons were coincident with those of reference [32]. This was because that more DA and PEI deposited on the surface of PVDF membrane at the same scope of time with the increase of the content of DA + PEI, which made the selective layer more thick and more porous. From Fig. 11 it can be found that the water flux decreased from 38.5 to 13.4 L m^{-2} h^{-1} bar^{-1}, while the PEG1000 rejection increased from 87.5% to 99.2% when the content of DA + PEI increased from 2 to 4 g L^{-1} (Fig. 11a). The reasons were that both the filtration resistance and the rejection capability increased with the increase of the selective thickness.

3.6. Performance and stability of PA/PDA/PVDF nanocomposite membranes in the simulating RB5 dyeing wastewater treatment

3.6.1. Performance of PA/PDA/PVDF nanocomposite membranes in the simulating RB5 dyeing wastewater treatment

Effects of the co-deposition time, mass ratio of DA to PEI, the molecular weight of PEI and the content of DA + PEI on the performance of PA/PDA/PVDF nanocomposite membranes in the simulating RB5 dyeing
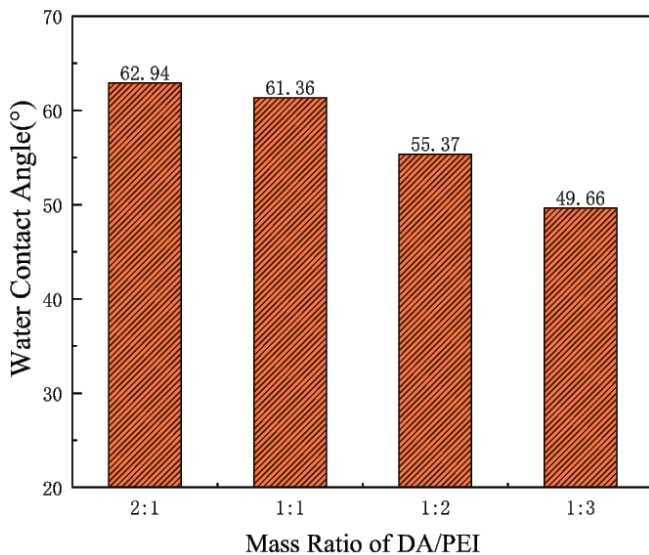

Fig. 6. Effects of the mass ratio of DA to PEI on the water contact angle of the PA/PDA/PVDF nanocomposite membranes.
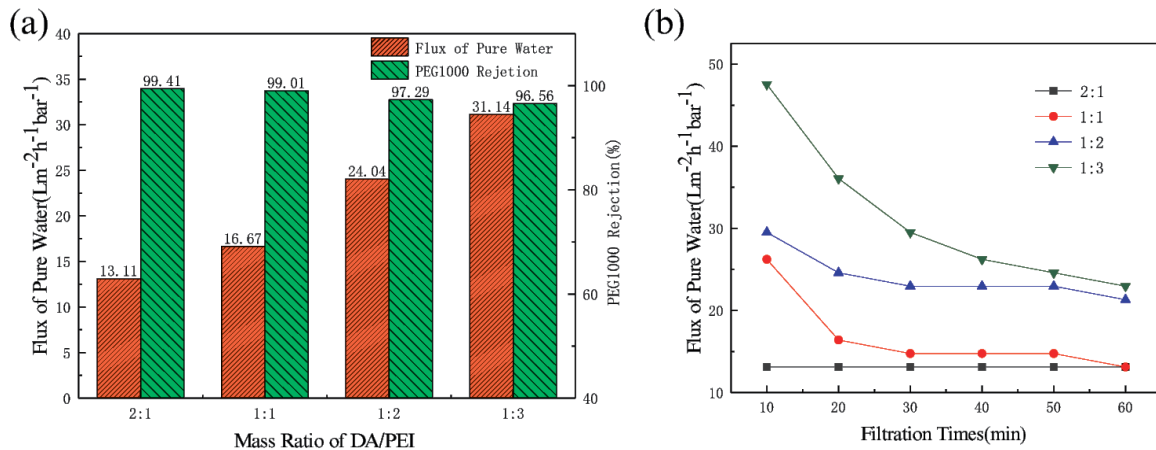

Fig. 7. Effects of the mass ratio of DA to PEI on the performance of PA/PDA/PVDF nanocomposite membranes: (a) the water flux and PEG1000 rejection and (b) the variety of the water flux with time.
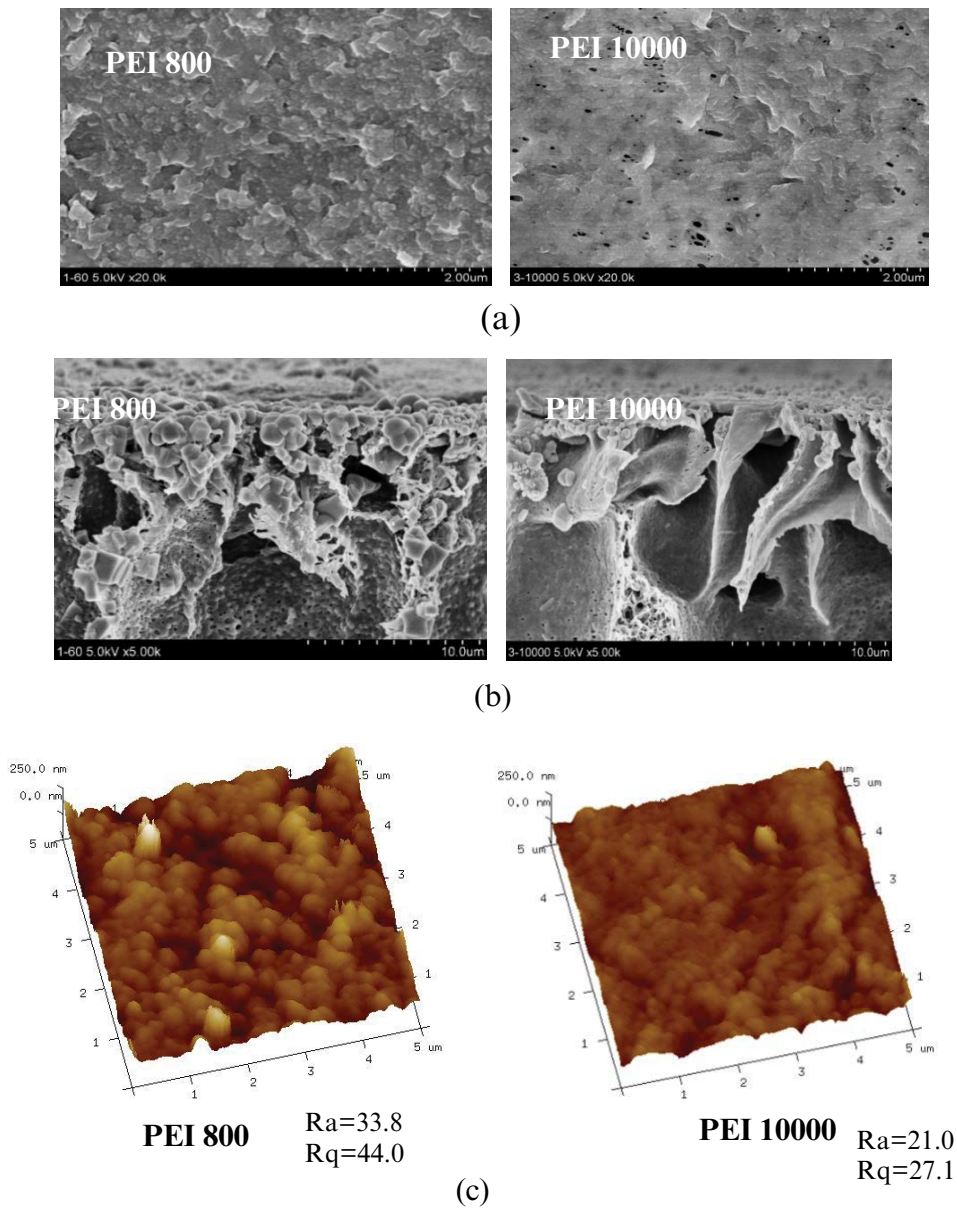
Fig. 8. Effects of the molecular weight of PEI on the morphologies of (a) the surface and (b) the cross-section and (c) the surface roughness of PA/PDA/PVDF nanocomposite membranes.
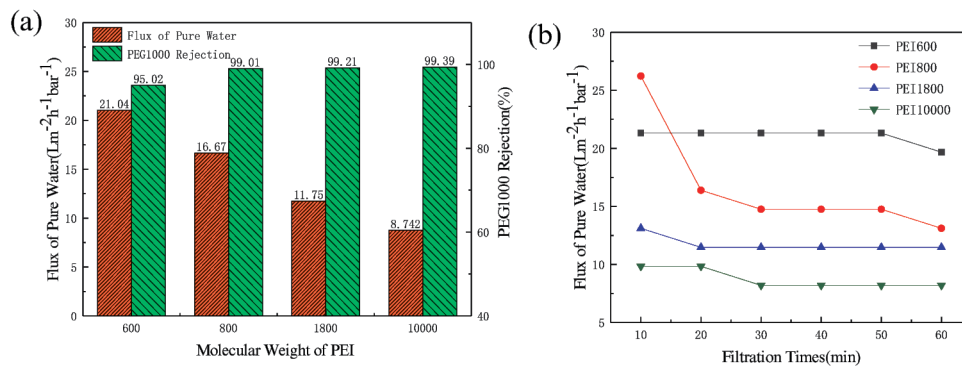

Fig. 9. Effects of the molecular weight of PEI on the performance of PA/PDA/PVDF nanocomposite membranes: (a) the water flux and PEG1000 rejection and (b) the variety of the water flux with time.
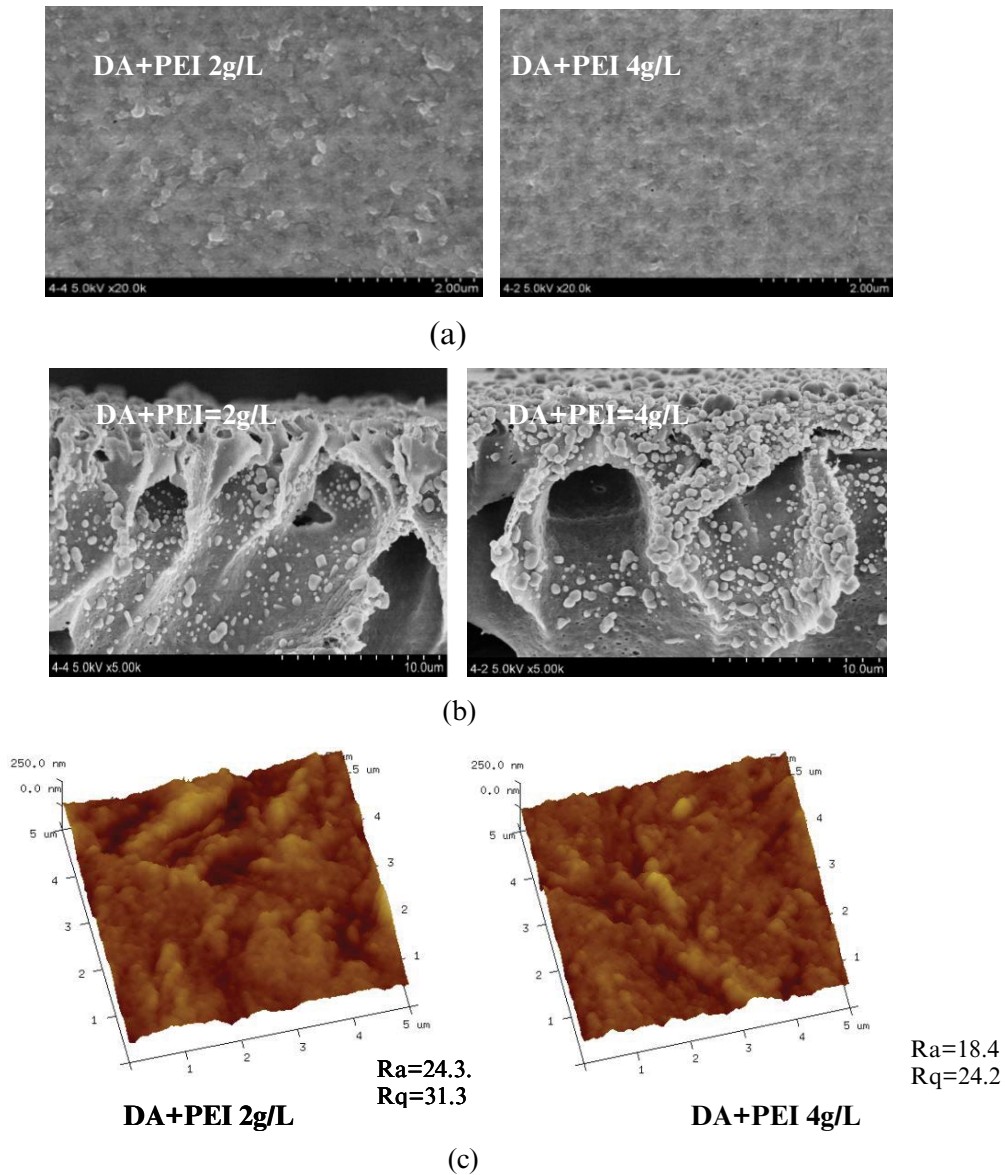
(a)

(b)

(c)

Fig. 10. Effects of the content of DA + PEI on the morphologies of (a) the surface and (b) the cross-section and (c) the surface roughness of PA/PDA/PVDF nanocomposite membranes.
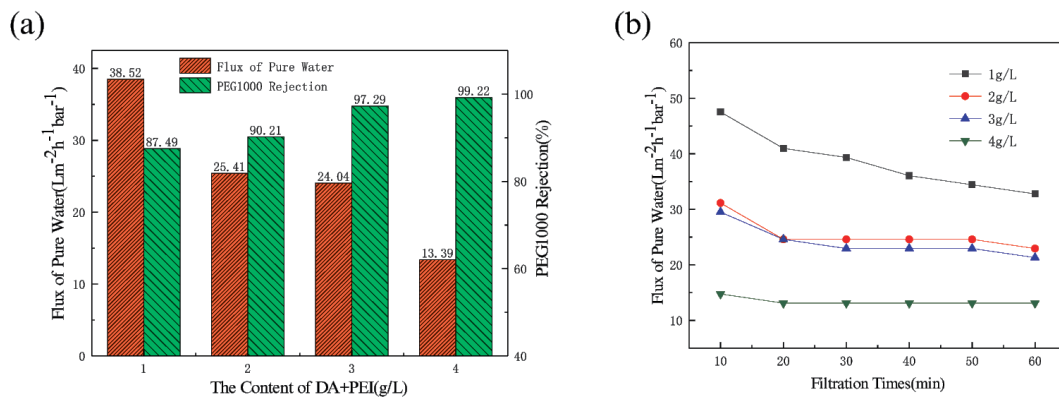

Fig. 11. Effects of the content of DA + PEI on the performance of PA/PDA/PVDF nanocomposite membranes: (a) the water flux and PEG1000 rejection and (b) the variety of the water flux with time.

wastewater treatment are displayed in Figs. 12-15, respectively. Figs. 12–15 show that the tendency of the simulating RB5 dyeing wastewater permeation and the RB5 rejection of PA/PDA/PVDF nanocomposite membranes were close to those of the pure water permeation and the PEG1000 rejection. From Fig. 14a it was found that the simulating RB5 dyeing wastewater permeation can be up to 15.03 L m^{-2} h^{-1} bar^{-1} when the RB5 rejection was above 93% at the condition of the co-deposition time 40 min, the mass ratio of DA to PEI 1:1, the molecular weight of PEI 600 and the content of DA + PEI 2 g L^{-1}. On the other hand, when the simulating RB5 dyeing wastewater permeation was 8.2 L m^{-2} h^{-1} bar^{-1}, the RB5 rejection can be up to 99% at the condition of the co-deposition time 40 min, the mass ratio of DA to PEI 1:1, the molecular weight of PEI 1800 and the content of DA + PEI 2 g L^{-1}, which can

be found in Fig. 13a. The results above stated that the PA/PDA/PVDF nanocomposite membranes developed in this work can reclaim the RB5 from the simulating RB5 dyeing wastewater effectively.

3.6.2. Operating stability of the PA/PDA/PVDF nanocomposite membranes in the simulating RB5 dyeing wastewater treatment

The varieties of the nanocomposite membranes permeation with time were used to tell whether the selective layer sticks on the base membranes firmly. If the permeation increases deeply, then the selective layer may detach from the base membranes. Fig. 16 displays the varieties of the permeation of PA/PDA/PVDF nanocomposite membranes, prepared at four different conditions, with
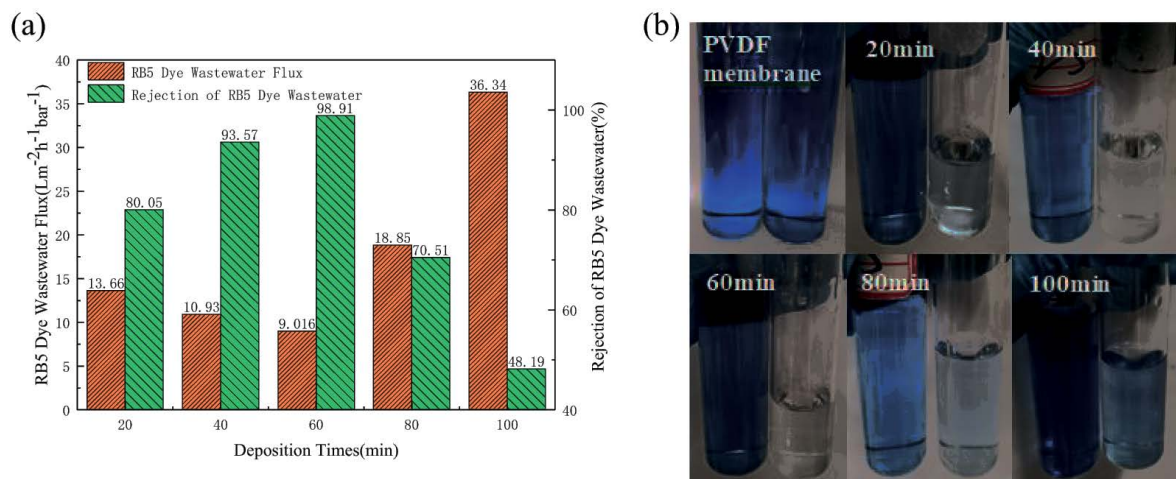

Fig. 12. Effects of the co-deposition time on the performance of the PA/PDA/PVDF nanocomposite membranes in the simulating RB5 dyeing wastewater treatment: (a) the permeation of the simulating RB5 dyeing wastewater and the RB5 rejection and (b) photos of feed solution and permeate solution.
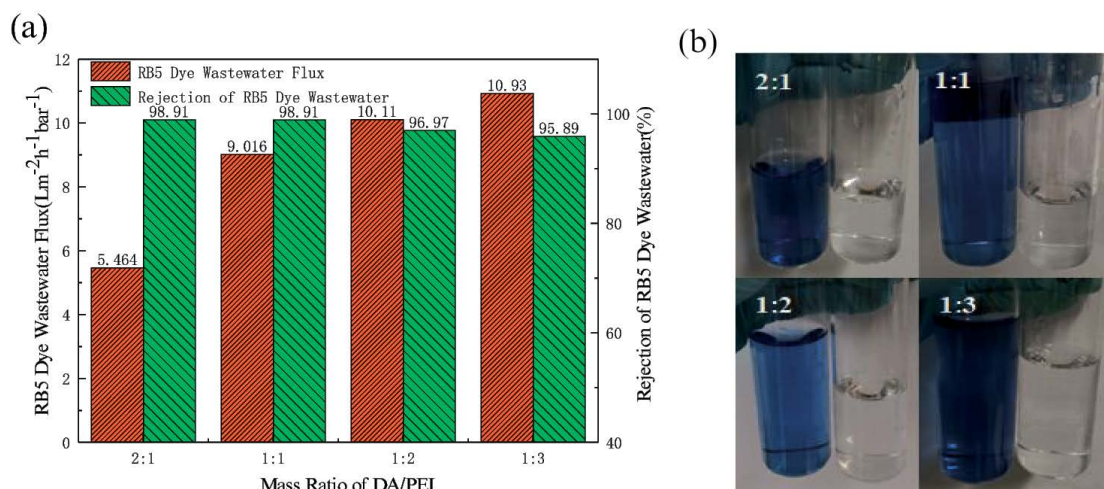

Fig. 13. Effects of the mass ratio of DA to PEI on the performance of the PA/PDA/PVDF nanocomposite membranes in the simulating RB5 dyeing wastewater treatment: (a) the permeation of the simulating RB5 dyeing wastewater and the RB5 rejection and (b) photos of feed solution and permeate solution.

(a)

(b)

Fig. 14. Effects of the molecular weight of PEI on the performance of the PA/PDA/PVDF nanocomposite membranes in the simulating RB5 dyeing wastewater treatment: (a) the permeation of the simulating RB5 dyeing wastewater and the RB5 rejection and (b) photos of feed solution and permeate solution.

(a)

(b)

Fig. 15. Effects of the molecular weight of PEI on the performance of the PA/PDA/PVDF nanocomposite membranes in the simulating RB5 dyeing wastewater treatment: (a) the permeation of the simulating RB5 dyeing wastewater and the RB5 rejection and (b) photos of feed solution and permeate solution.
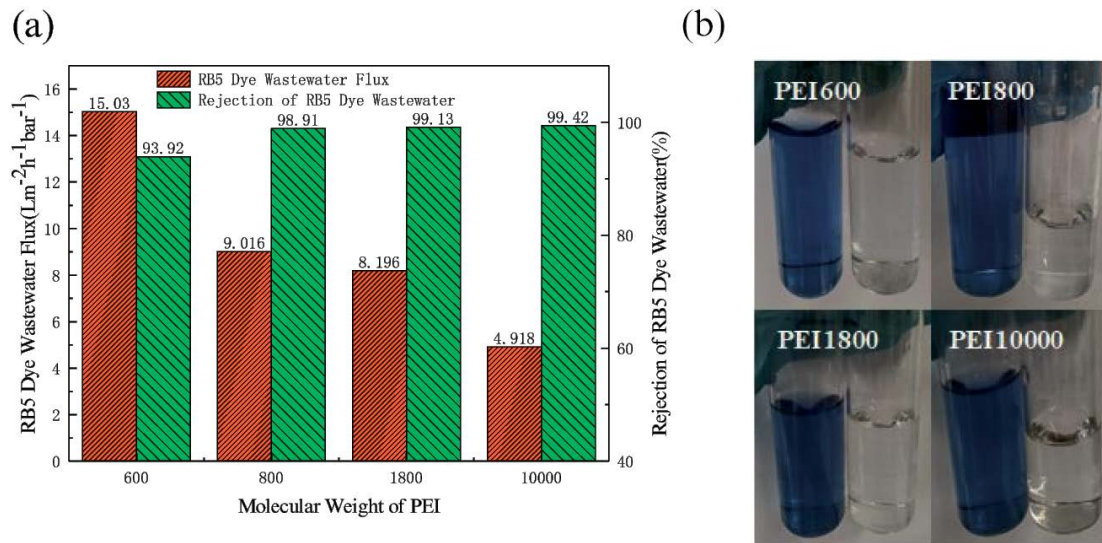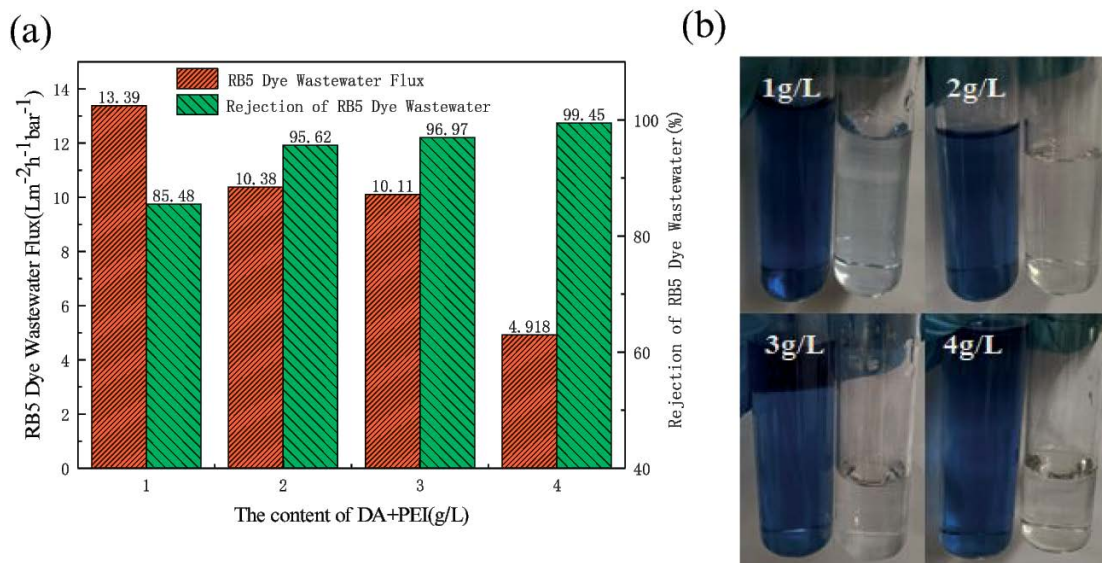
time in the simulating RB5 dyeing wastewater treatment within 6 h. From Fig. 16 it can be found that neither of the perpeation of the membranes at four different conditions increased drastically. On the contrary, the perpeation of the membranes at the condition of the mass ratio of DA to PEI 2:1 and the content of DA + PEI 4 g L^{-1} were steady with time, and the permeation at the condition of co-deposition time 60 min and the molecular weight of PEI 10000 decreased vertically at 4 and 5 h, respectively, then kept stable. The results of Fig. 16 mean that the selective layer of the four PA/PDA/PVDF nanocomposite membranes all sticked with the base membranes firmly, the decrease of permeation were due to the filtration resistance

resulted by the membrane fouling in the operation but not the detatchment of the selective layer.

4. Conclusion

According to the above results and discussions, the following conclusions can be drawn: The permeation increases with the decrease of the mass ratio of DA to PEI, the molecular weight of PEI and the content of DA + PEI, while, the permeation decreases first, then increases with co-deposition time, the rejection is just opposite of that tendency. Considering the permeation and the rejection, the optimum co-deposition time is chosen as 40 min. Within the scope of
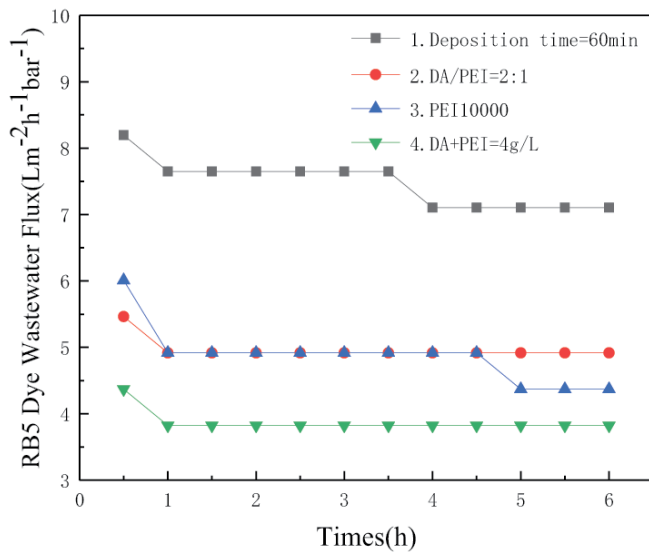
Fig. 16. Operating stability of the PA/PDA/PVDF nanocomposite membranes in the simulating RB5 dyeing wastewater treatment.

investigation, the water flux and the RB5 dyeing wastewater permeation were 31.14 and 15.03 L m^{-2} h^{-1} bar^{-1}, respectively, when the PEG1000 and RB5 rejection were above 90%. When the rejection of PEG1000 and RB5 were 99%, the permeation of water and RB5 dyeing wastewater were 16.67 and 8.2 L m^{-2} h^{-1} bar^{-1}, respectively.

References

[1] D. Nayeri, S.A. Mousavi, Dye removal from water and wastewater by nanosized metal oxides modified activated carbon: a review on recent research, J. Environ. Health Sci. Eng., 18 (2020) 1671–1689.

[2] S. Samsami, M. Mohamadizaniani, M.-H. Sarrafzadeh, E.R. Rene, Recent advances in the treatment of dye-containing wastewater from textile industries: overview and perspectives, Process Saf. Environ. Prot., 143 (2020) 138–163.

[3] Q. Li, Z.P. Liao, X.F. Fang, D.P. Wang, J. Xie, X.Y. Sun, L.J. Wang, J.S. Li, Tannic acid-polyethyleneimine crosslinked loose nanofiltration membrane for dye/salt mixture separation, J. Membr. Sci., 584 (2019) 324–332.

[4] Y. Xiao, D.X. Guo, T. Li, Q.F. Zhou, L.G. Shen, R.J. Li, Y.C. Xu, H.J. Lin, Facile fabrication of superhydrophilic nanofiltration membranes via tannic acid and irons layer-by-layer self-assembly for dye separation, Appl. Surf. Sci., 515 (2020) 146063, doi: 10.1016/j.apsusc.2020.146063.

[5] Y. Xu, Z.H. Li, K.M. Su, T.T. Fan, L. Cao, Mussel-inspired modification of PPS membrane to separate and remove the dyes from the wastewater, Chem. Eng. J., 341 (2018) 371–382.

[6] X.-L. Cao, Y.-N. Yan, F.-Y. Zhou, S.-P. Sun, Tailoring nanofiltration membranes for effective removing dye intermediates in complex dye-wastewater, J. Membr. Sci., 595 (2020) 117476, doi: 10.1016/j.memsci.2019.117476.

[7] F. Oulad, S. Zinadini, A.A. Zinatizadeh, A.A. Derakhshan, Fabrication and characterization of a novel tannic acid coated boehmite/PES high performance antifouling NF membrane and application for licorice dye removal, Chem. Eng. J., 397 (2020) 125105, doi: 10.1016/j.cej.2020.125105.

[8] S. Sakarkar, S. Muthukumaran, V. Jegatheesan, Evaluation of polyvinyl alcohol (PVA) loading in the PVA/titanium dioxide (TiO$_2$) thin film coating on polyvinylidene fluoride (PVDF) membrane for the removal of textile dyes, Chemosphere, 257 (2020) 127144, doi: 10.1016/j.chemosphere.2020.127144.

[9] W.Y. Ye, K.F. Ye, F. Lin, H.W. Liu, M. Jiang, J. Wang, R. Liu, J.Y. Lin, Enhanced fractionation of dye/salt mixtures by tight ultrafiltration membranes via fast bio-inspired co-deposition for sustainable textile wastewater management, Chem. Eng. J., 379 (2020) 122321, doi: 10.1016/j.cej.2019.122321.

[10] F.-F. Ma, D. Zhang, N. Zhang, T. Huang, Y. Wang, Polydopamine-assisted deposition of polypyrrole on electrospun poly(vinylidene fluoride) nanofibers for bidirectional removal of cation and anion dyes, Chem. Eng. J., 354 (2018) 432–444.

[11] M.T. Hoang, T.D. Pham, D. Verheyen, M.K. Nguyen, T.T. Pham, J.Y. Zhu, B.V. der Bruggen, Fabrication of thin film nanocomposite nanofiltration membrane incorporated with cellulose nanocrystals for removal of Cu(II) and Pb(II), Chem. Eng. Sci., 228 (2020) 115998, doi: 10.1016/j.ces.2020.115998.

[12] M.B.M. Yap Ang, C.-L. Tang, M.R. De Guzman, H.L.C. Maganto, A.R. Caparanga, S.-H. Huang, H.-A. Tsai, C.-C. Hu, K.-R. Lee, J.-Y. Lai, Improved performance of thin-film nanofiltration membranes fabricated with the intervention of surfactants having different structures for water treatment, Desalination, 481 (2020) 114352, doi: 10.1016/j.desal.2020.114352.

[13] M.B. He, T. Li, M. Hu, C. Chen, B.C. Liu, J. Crittenden, L.-Y. Chu, H.Y. Ng, Performance improvement for thin-film composite nanofiltration membranes prepared on PSf/PSf-g-PEG blended substrates, Sep. Purif. Technol., 230 (2020) 115855, doi: 10.1016/j.seppur.2019.115855.

[14] S. Ghiasi, A. Behboudi, T. Mohammadi, M. Ulbricht, High-performance positively charged hollow fiber nanofiltration membranes fabricated via green approach towards polyethyleneimine layer assembly, Sep. Purif. Technol., 251 (2020) 117313, doi: 10.1016/j.seppur.2020.117313.

[15] G.C. Li, B. Liu, L.M. Bai, Z. Shi, X.B. Tang, J. Wang, H. Liang, Y.T. Zhang, B.V. der Bruggen, Improving the performance of loose nanofiltration membranes by poly-dopamine/zwitterionic polymer coating with hydroxyl radical activation, Sep. Purif. Technol., 238 (2020) 116412, doi: 10.1016/j.seppur.2019.116412.

[16] K. Shen, P.Y. Li, T.H. Zhang, X.F. Wang, Salt-tuned fabrication of novel polyamide composite nanofiltration membranes with three-dimensional turing structures for effective desalination, J. Membr. Sci., 607 (2020) 118153, doi: 10.1016/j.memsci.2020.118153.

[17] L. Ren, J.X. Chen, Q. Lu, C.B. Wang, J. Han, K. Huang, X.N. Pan, H. Wu, Construction of high selectivity and antifouling nanofiltration membrane via incorporating macrocyclic molecules into active layer, J. Membr. Sci., 597 (2020) 117641, doi: 10.1016/j.memsci.2019.117641.

[18] J. Wang, J.Y. Zhu, M.T. Tsehaye, J. Li, G.Y. Dong, S.S. Yuan, X. Li, Y.T. Zhang, J.D. Liu, B.V. der Bruggen, High flux electroneutral loose nanofiltration membranes based on rapid deposition of polydopamine/polyethyleneimine, J. Mater. Chem., A, 5 (2017) 14847–14857.

[19] R.N. Zhang, Y.L. Su, X.T. Zhao, Y.F. Li, J.J. Zhao, Z.Y. Jiang, A novel positively charged composite nanofiltration membrane prepared by bio-inspired adhesion of polydopamine and surface grafting of poly(ethylene imine), J. Membr. Sci., 470 (2014) 9–17.

[20] J.Q. Li, A.Q. Tang, J.Y. Lu, P.B. Zhang, M.X. Shen, L.P. Zhu, Effects of extra amine sources on the permeability and separation properties of nanofiltration membranes prepared by polydopamine deposition, Desal. Water Treat., 147 (2019) 10–19.

[21] R.J. Li, J.X. Liu, A. Shi, X.Q. Luo, J.C. Lin, R. Zheng, H.X. Fan, S.V. Selasie, A facile method to modify polypropylene membrane by polydopamine coating via inkjet printing technique for superior performance, J. Colloid Interface Sci., 552 (2019) 719–727.

[22] H.Q. Wu, J.D. Xie, L. Mao, One-pot assembly tannic acid-titanium dual network coating for low-pressure nanofiltration membranes, Sep. Purif. Technol., 233 (2020) 116051, doi: 10.1016/j.seppur.2019.116051.

[23] H.X. Guo, S.C. Yu, T.T. Liu, Q.F. An, X.Y. Ren, Z.P. Qin, Y.C. Liang, Counterion-switched reversibly hydrophilic and hydrophobic TiO$_2$-incorporated layer-by-layer self-assembled membrane for nanofiltration, Macromol. Mater. Eng., 304 (2019) 1900481, doi: 10.1002/mame.201900481.

[24] Y.H. Xiang, F. Liu, L.X. Xue, Under seawater superoleophobic PVDF membrane inspired by polydopamine for efficient oil/ seawater separation, J. Membr. Sci., 476 (2015) 321–329.

[25] H. Shi, Y. He, Y. Pan, H.H. Di, G.Y. Zeng, L. Zhang, C.L. Zhang, A modified mussel-inspired method to fabricate TiO_2 decorated superhydrophilic PVDF membrane for oil/water separation, J. Membr. Sci., 506 (2016) 60–70.

[26] G.H. Zin, J.J. Wu, K. Rezzadori, J.C.C. Petrus, M. Di Luccio, Q.L. Li, Modification of hydrophobic commercial PVDF microfiltration membranes into superhydrophilic membranes by the mussel-inspired method with dopamine and polyethyleneimine, Sep. Purif. Technol., 212 (2019) 641–649.

[27] H.-C. Yang, M.-B. Wu, Y.-J. Li, Y.-F. Chen, L.-S. Wan, Z.-K. Xu, Effects of polyethyleneimine molecular weight and proportion on the membrane hydrophilization by codepositing with dopamine, J. Appl. Polym. Sci., 133 (2016) 43792, doi: 10.1002/app.43792.

[28] H.-M. Song, C. Chen, X.-X. Shui, H. Yang, L.-J. Zhu, Z.-X. Zeng, Q.-J. Xue, Asymmetric Janus membranes based on in situ mussel-inspired chemistry for efficient oil/water separation, J. Membr. Sci., 573 (2019) 126–134.

[29] P.-B. Zhang, C.-J. Liu, J. Sun, B.-K. Zhu, L.-P. Zhu, Fabrication of composite nanofiltration membranes by dopamine-assisted poly(ethylene imine) deposition and cross-linking, J. Zhejiang Univ.-Sci. A, 18 (2017) 138–150.

[30] J.Y. Zhu, S.S. Yuan, A. Uliana, J.W. Hou, J. Li, X. Li, M.M. Tian, Y. Chen, A. Volodin, B.V. der Bruggen, High-flux thin film composite membranes for nanofiltration mediated by a rapid co-deposition of polydopamine/piperazine, J. Membr. Sci., 554 (2018) 97–108.

[31] Y.-L. Ji, M.B.M.Y. Ang, H.-C. Hung, S.-H. Huang, Q.-F. An, K.-R. Lee, J.-Y. Lai, Bio-inspired deposition of polydopamine on PVDF followed by interfacial cross-linking with trimesoyl chloride as means of preparing composite membranes for isopropanol dehydration, J. Membr. Sci., 557 (2018) 58–66.

[32] Y. Lv, H.-C. Yang, H.-Q. Liang, L.-S. Wan, Z.-K. Xu, Nanofiltration membranes via co-deposition of polydopamine/polyethylenimine followed by cross-linking, J. Membr. Sci., 476 (2015) 50–58.

[33] M.M. Li, J. Xu, C.-Y. Chang, C.C. Feng, L. Zhang, Y.Y. Tang, C.J. Gao, Bioinspired fabrication of composite nanofiltration membrane based on the formation of DA/PEI layer followed by cross-linking, J. Membr. Sci., 459 (2014) 62–71.

[34] Y.F. Li, Y.L. Su, J.Y. Li, X.T. Zhao, R.N. Zhang, X.C. Fan, J.N. Zhu, Y.Y. Ma, Y. Liu, Z.Y. Jiang, Preparation of thin film composite nanofiltration membrane with improved structural stability through the mediation of polydopamine, J. Membr. Sci., 476 (2015) 10–19.

[35] R.J. Li, H.X. Fan, L.G. Shen, L.H. Rao, J.Y. Tang, S.F. Hu, H.J. Lin, Inkjet printing assisted fabrication of polyphenol-based coating membranes for oil/water separation, Chemosphere, 250 (2020) 126236, doi: 10.1016/j.chemosphere.2020.126236.

[36] R.J. Li, J.Y. Li, L.H. Rao, H.J. Lin, L.G. Shen, Y.C. Xu, J.R. Chen, B.-Q. Liao, Inkjet printing of dopamine followed by UV light irradiation to modify mussel-inspired PVDF membrane for efficient oil-water separation, J. Membr. Sci., 619 (2021) 118790, doi: 10.1016/j.memsci.2020.118790.

[37] M.-B. Wu, X.-L. Fan, H.-C. Yang, J. Yang, M.-M. Zhu, K.-F. Ren, J. Ji, Z.-K. Xu, Ultrafast formation of pyrogallol/polyethyleneimine nanofilms for aqueous and organic nanofiltration, J. Membr. Sci., 570–571 (2019) 270–277.

[38] Q.Q. Zeng, Y. Liu, L.G. Shen, H.J. Lin, W.M. Yu, Y.C. Xu, R.J. Li, L.L. Huang, Facile preparation of recyclable magnetic Ni@filter paper composite materials for efficient photocatalytic degradation of methyl orange, J. Colloid Interface Sci., 582 (2021) 291–300.

[39] Y. Long, G.Y. Yu, D. Lu, Y.C. Xu, H.J. Lin, Y. Deng, X.J. You, L.N. Yang, B.-Q. Liao, Synergistic fouling behaviors and mechanisms of calcium ions and polyaluminum chloride associated with alginate solution in coagulation-ultrafiltration (UF) process, Water Res., 189 (2021) 116665, doi: 10.1016/j.watres.2020.116665.

[40] Y. Deng, X.L. Zhou, J. Shen, G. Xiao, H.C. Hong, H.J. Lin, F.Y. Wu, B.-Q. Liao, New methods based on back propagation (BP) and radial basis function (RBF) artificial neural networks (ANNs) for predicting the occurrence of haloketones in tap water, Sci. Total Environ., 772 (2021) 145534, doi: 10.1016/j.scitotenv.2021.145534.

[41] Z.Y. Huang, J.H. Liu, Y. Liu, Y.C. Xu, R.J. Li, H.C. Hong, L.G. Shen, H.J. Lin, B.-Q. Liao, Enhanced permeability and antifouling performance of polyether sulfone (PES) membrane via elevating magnetic Ni@MXene nanoparticles to upper layer in phase inversion process, J. Membr. Sci., 623 (2021) 119080, doi: 10.1016/j.memsci.2021.119080.

[42] Y.R. Xiao, W.T. Zhang, Y. Jiao, Y.C. Xu, H.J. Lin, Metal-phenolic network as precursor for fabrication of metal-organic framework (MOF) nanofiltration membrane for efficient desalination, J. Membr. Sci., 624 (2021) 119101, doi: 10.1016/j.memsci.2021.119101.